

# Examining Hemispheric Asymmetries in Field-Aligned Currents at Earth Using Ground-Based Data

J. Kay, J. Coxon

## Key Points:

- The atmosphere impacts ionospheric currents such that asymmetries between the hemispheres are exaggerated compared to space-based data
- Ground-based field-aligned currents were on average roughly 3 times stronger in the Northern Hemisphere than in the South
- Both hemispheres exhibit signs consistent with positive IMF  $B_y$  despite observations showing no overall trend in  $B_y$  over our dataset

## Abstract

We use measurements from the ground-based Spherical Elementary Current (SEC) dataset to compare the field-aligned currents (FACs) in the Earth's Northern and Southern Hemispheres over the years 2015 and 2016. We use Altitude-Adjusted Corrected Geomagnetic (AACGM) and Magnetic Local Time (MLT) coordinate systems to compile maps of the FACs on Earth during all days of this dataset. With this data we calculate the Asymmetry Index (AI) between the hemispheres, both overall for the entire time frame, and for individual daily maps. Over these two years we found the Asymmetry Index to vary with a period of roughly 1 year and amplitude of  $\sim 0.4$ , with the maxima and minima lying on Northern and Southern summer respectively. Over the spring equinoxes in 2015/2016 we found currents in the Northern Hemisphere to over 3 times higher on average than those in the Southern Hemisphere. We also noticed a consistent clockwise rotation of the polar current regions, which would be indicative of a constantly positive  $B_y$  component of the Interplanetary Magnetic Field (IMF) over the 2 year time period although this is not reflected in space-based IMF observations, this rotation was most evident during the 2016 spring equinox. The differences between this dataset and previous space-based observations may be explained due to interference from the Earth's atmosphere though further investigation is needed to determine an exact explanation.

## 1 Background

Field-aligned currents (FACs) represent a fundamental component of the interaction between the Earth's magnetosphere and ionosphere, playing a pivotal role in transferring energy between different regions of the Earth's magnetic field. The generation and evolution of these currents are affected by various space weather phenomena, producing asymmetries in the currents between Earth's two hemispheres. There are also various interactions between the Earth's atmosphere and these ionospheric currents which create imbalances between the hemispheres, many of the mechanisms behind these asymmetries are not fully understood.

At the Earth's poles, due to the nature of reconnection in the Earth's magnetic field, regions of positive (upward) and negative (downward) field-aligned currents emerge. Reconnection occurs when the magnetic field lines from different regions with opposing orientations come into contact, allowing charged particles, which would normally be frozen-in to the magnetic fields, to move freely between the field lines. These particles then move parallel to the field lines producing currents (S. W. H. Cowley 2000). The formation of different regions of current are related to the effects of the Hall and Pedersen currents, induced by the Earth's magnetic field.

The Hall current is a perpendicular current that flows in response to the electric field generated by the relative motion between the ionospheric plasma and the geomagnetic field. It arises due to the Lorentz force acting on charged particles moving perpendicular to both the magnetic field lines and the electric field. This current flows perpendicular to the magnetic and electric field lines. Additionally at altitudes below  $\sim 125$ km ions have a higher collision frequency than electrons (S. W. H. Cowley 2000), causing a charge separation in the plasma flow and meaning the Hall current is driven partially by ions colliding more frequently than electrons.

Pedersen currents emerge due to the interaction between charged particles in motion and neutrals under the influence of a magnetic field. Due to the nature of charged particle gyration in magnetic fields, after a collision with a neutral, this gyration is essentially reset resulting in the charged particle being more likely to move with the field if positively charged, or against the field if negatively charged. In the ionosphere ion collision frequency is roughly equal to gyration frequency at  $\sim 125$ km above the Earth's surface (Stanley W. H. Cowley 2007), as electrons are significantly lighter than protons, hav-

ing a larger gyration frequency, they are able to move faster, resulting in charge separation and a current in the positive direction of the electric field lines.

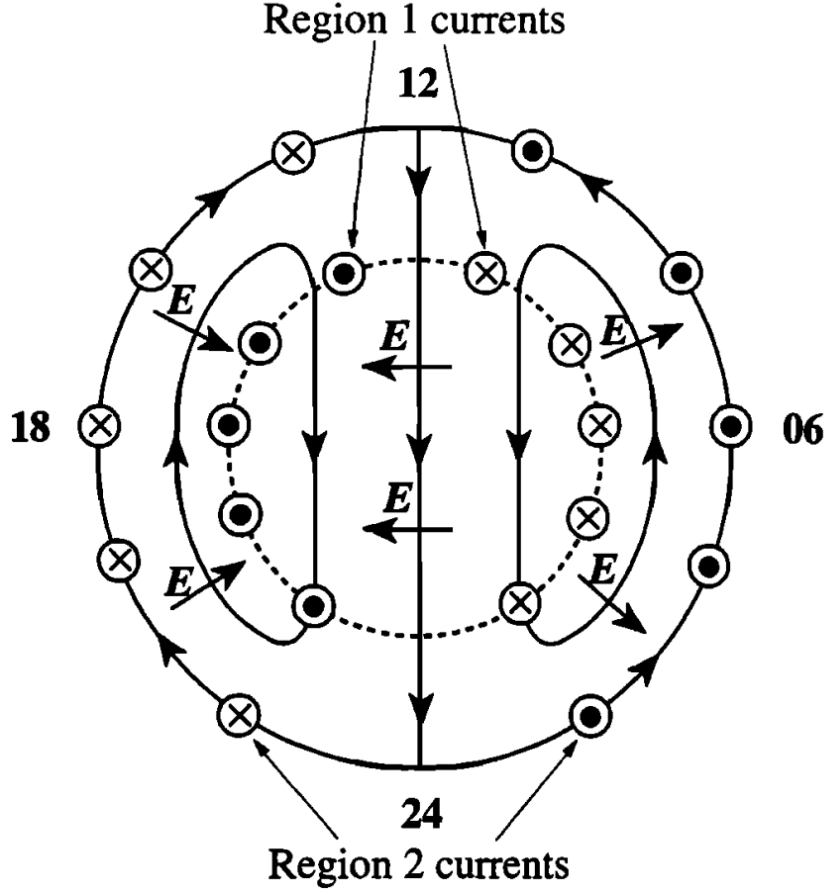


**Figure 1.** A schematic of the plasma flows mapped on to the Earth's poles (S. W. H. Cowley 2000). The solid arrowed lines forming loops are the plasma streamlines which flow opposite to the Hall current, while the shorter arrows represent the electric field and the direction of flow of the Pedersen currents. Field-aligned currents flow as depicted by the magnetic fields.

In the context of the Earth's magnetic field near the poles, Hall currents produce current loops parallel to the Earth's surface with currents nearer the pole moving in the direction of the sun which loop around, moving toward the equator and toward the night side of the Earth before completing the loop. This can be seen in Figure 1 where the Hall currents flow in the opposite direction to the plasma streamlines. Pedersen currents on the other hand, being parallel to electric field, flow to and from the loops formed by the Hall currents, which are perpendicular to the ionospheric plasma flow, again depicted in Figure 1. The currents which flow directly along the Earth's magnetic field lines form the field-aligned currents and are a resource which can be used to measure the magnitude of the Earth's ionosphere from the surface (S. W. H. Cowley 2000).

Under nominal conditions this results in 2 major polar regions split along a central line from 12 - 24 hours, with region 1 representing the field-aligned currents entering the Earth at the centre of the Hall current loops on either side of the Earth's dipole, and region 2 being the field-aligned currents nearer the equator outside of these loops.

Region 1 lies at roughly  $75^\circ$  North and South with the positive half of the region generally lying at the side of the Earth nearer dusk and the negative half lying at the dawn side. Region 2 has these currents reversed and lies at roughly  $60^\circ$  from the equator, these regions are depicted in Figure 2 with respect to the Earth's field lines (J. C. Coxon et al. 2016). From observations we see that the strength, size, and angle between these regions are governed by several factors (S. W. H. Cowley 2000, Davey et al. 2012), many of which have directly inverse effects between the Northern and Southern Hemispheres causing quantifiable asymmetries in the field-aligned currents at the poles. These asymmetries may manifest as changes in field magnitude, rotations of the current regions, or changes in size of the regions, depending on the type of ionospheric interference.

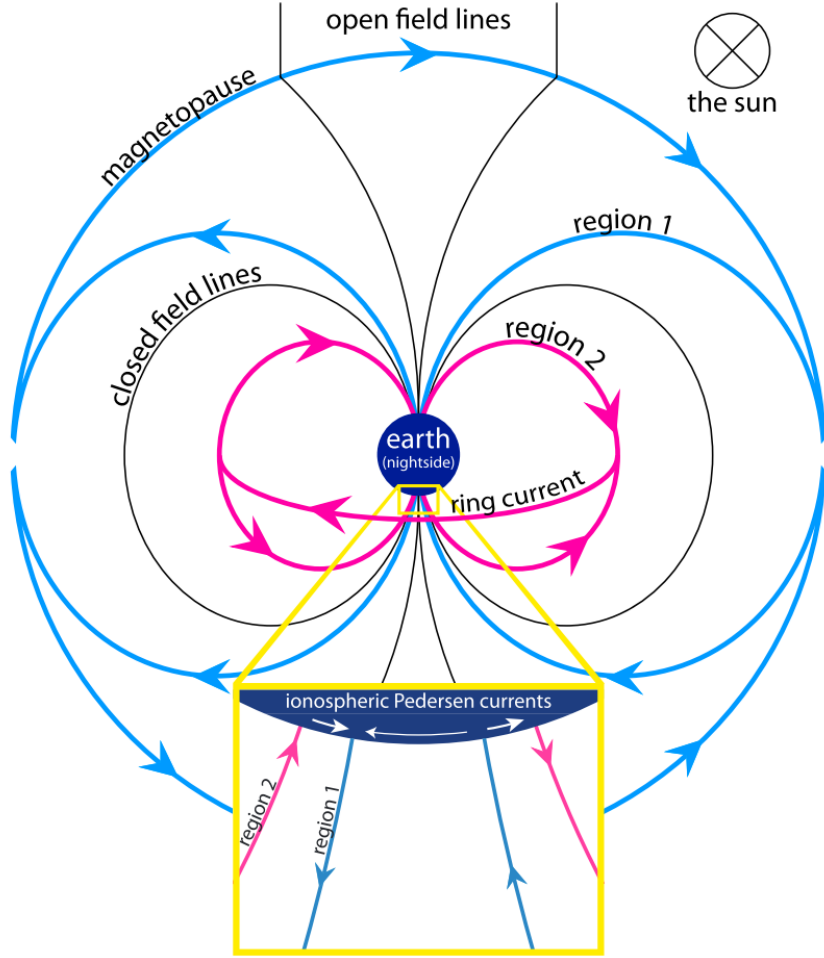


**Figure 2.** Diagram of the Earth, viewed from the nightside, displaying the regions of current in relation to the Earth's magnetosphere (J. C. Coxon et al. 2016).

Perhaps the largest asymmetry which effects the Earth's ionosphere is that of the seasonal changing inclination of the Earth's axis due to its orbit around the sun (S. W. H. Cowley 2000, Workayehu, Vanhamäki, and Aikio 2020). During different seasons the angle at which solar radiation strikes the ionosphere varies between the hemispheres leading to more incident radiation in the Northern Hemisphere during Northern summer and vice versa. During summer this increased solar radiation enhances ionization and conductivity in the ionosphere leads to stronger ionospheric currents compared to the win-

ter hemisphere. This asymmetry is significantly reduced during equinoxes, when the axis of Earth is neither inclined toward nor away from the Sun, this results in the distribution of field-aligned currents tending to be relatively symmetric between the Northern and Southern Hemispheres.

The  $B_y$  component of the Interplanetary Magnetic Field (IMF) also produces some asymmetries in the ionospheric currents of Earth's hemispheres. This component of the magnetic field lies in the magnetic equatorial plane, perpendicular to the magnetic dipole, as expressed in geocentric solar coordinates (GSM), inducing an East-West asymmetry in the ionospheric currents. The asymmetry arises due to the  $B_y$  fields causing a twisting of the angle between the fields in the magnetotail current sheet which propagates to the Earth's poles causing a rotation in the observed current regions from a low  $B_y$  case (Weimer 2001, Davey et al. 2012). Consequently, the ionospheric conductivity and electric field strength vary between the Northern and Southern Hemispheres due to the differing magnetic field strengths and orientations. As a result, the ionospheric currents exhibit asymmetries, causing the angle through the magnetic pole between the two halves of each region to rotate depending on the sign of  $B_y$ . Positive values  $B_y$  cause the axis to shift clockwise from the Northern perspective, with negative values causing an anti-clockwise rotation. Due to the nature of the twisting in the magnetotail these rotations are opposite in both hemispheres as can be seen in Figure 3 (J. M. Weygand et al. 2023).

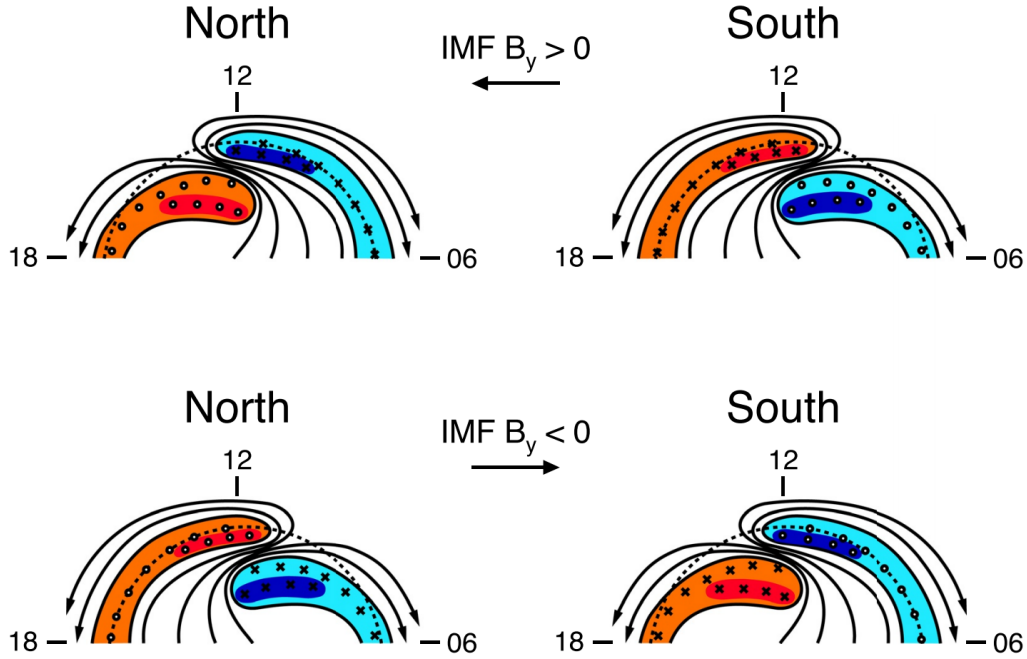


**Figure 3.** Field-aligned current patterns under positive and negative IMF  $B_y$ . Red indicates upward positive currents and blue indicates downward negative currents (J. M. Weygand et al. 2023).

Asymmetries also arise due to diurnal variation, driven by the asymmetrical distribution of solar radiation over the course of a 24 hour day. As Earth rotates on its axis, different regions of the ionosphere experience varying degrees of solar radiation, during local daytime, when solar radiation is more intense, ionization levels are higher, leading to increased conductivity in the ionosphere (Merrill, McElhinny, and McFadden 1998).

Additionally, as the geomagnetic and geographic poles are not aligned, with the geomagnetic pole rotating around the geographic with the Earth’s spin, leading to the location of incident radiation interacting with the magnetic field at further varying locations throughout each day.

These asymmetries have been observed in space-based data such as that from the Active Magnetosphere and Planetary Electrodynamics Response Experiment (AMPERE) which, between 2010 and 2015 indicated more current flowed in the Northern Hemisphere during Northern summer and vice versa (J. C. Coxon et al. 2016, John C. Coxon et al. 2022). These observations also confirm expected diurnal variations with currents varying as expected over the course of each day.

The paper from J. C. Coxon et al. 2016 also provides evidence of unexplained consistent systematically higher currents on average flowing through the Northern Hemisphere, suggesting that the Northern Hemisphere may have a stronger reaction to day-side reconnection than the Southern Hemisphere. This has also been observed in data from the Swarm satellites by Workayehu, Vanhamäki, and Aikio 2019, which measures field-aligned currents in the Northern Hemisphere to be higher by  $12 \pm 4\%$  on average than currents in the Southern Hemisphere, though they also state that asymmetries are lower in conditions with higher reconnection. Observations from Swarm satellites also display these higher Northern currents, indicating a maximum ratio of field-aligned currents between the hemispheres in local autumn of  $1.16 \pm 0.07$  (Workayehu, Vanhamäki, Aikio, and Shepherd 2021).

Other data from Swarm satellite observations also display the additional unexplained seasonal asymmetry with a maximum ratio of field-aligned currents between the hemispheres being highest in winter at  $1.15 \pm 0.05$ , dropping to  $1.04 \pm 0.04$  in summer (Workayehu, Vanhamäki, and Aikio 2020). These observations also note an additional diurnal asymmetry where the ratio in currents between the North and South Hemispheres was higher during the evening than in the morning.

These asymmetries in the field-aligned current magnitudes have not been reproduced with ground-based data and so further investigation will allow for more insight to be gained into the exact causes of these unexplained Hemispheric asymmetries. Investigation into ground-based data will also allow for the interaction between the atmosphere and field-aligned currents to be further quantified by comparing the differences between these observations and previous space-based data.

## 2 Methodology

For our analysis we use the Spherical Elementary Current (SEC) Amplitudes dataset (James M. Weygand et al. 2011), which provides current amplitudes at several locations in the Earth’s Northern and Southern Hemispheres over, at present, the years 2007 - 2022. The SECS technique involves measuring the magnetic field variation via ground-based magnetometers and using this variation to calculate the distribution and strength of atmospheric currents. This technique assumes that atmospheric currents can be represented as a collection of elementary currents distributed spherically around the Earth and works as a proxy for the field-aligned currents at the Earth’s surface (Amm and Viljanen 1999).

For our investigation we use SEC data from the years 2015 and 2016, as this is the only part of the SEC dataset which has data available in the Southern Hemisphere over a large time frame. Additionally we require the data from both hemispheres to be conjugate for our comparisons which is provided by this dataset. It should be noted that this dataset includes data from roughly 4 times more stations in the Northern Hemisphere and so has a smaller range of data from the Southern Hemisphere. The dataset also is missing various days worth of Southern data, with 453/731 days present over the 2 years,

this is particularly noticeable in Southern winter due to the difficulty of recording Antarctic data at those times of year.

As we are using SEC data, positive values for current indicate upward current flow defined in the positive Z direction and vice versa for negative currents, due to this and the nature of how SEC data is collected, values in the Southern Hemisphere have had their signs inverted to allow direct comparisons between the hemispheres. The location of each station which collects current amplitude data for the SEC dataset can be seen in Figure 4. The Northern bias in the data can be clearly seen here with 1012 stations in the North Hemisphere, and only 280 in the South. This figure also gives perspective on the size of the currents measured by this dataset which can reach up to  $\sim \pm 10^5$  A.

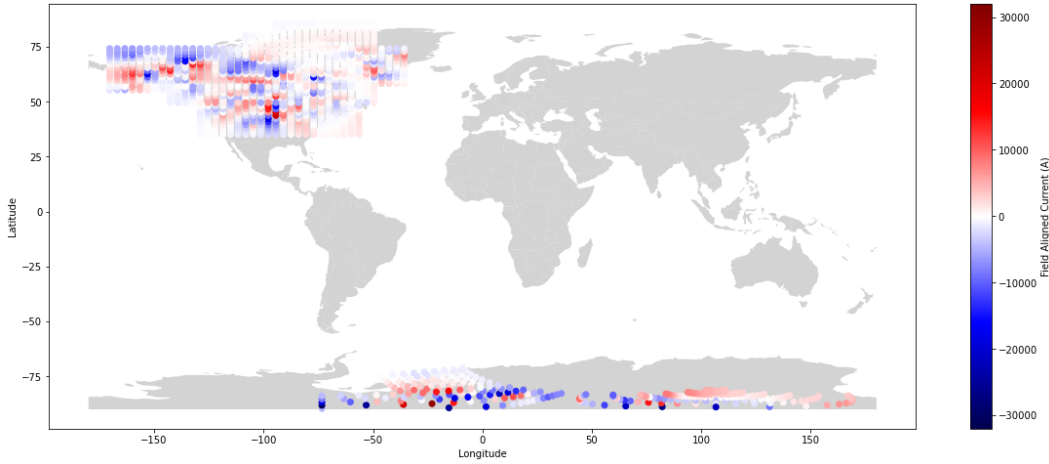


**Figure 4.** SEC field-aligned current amplitudes in both Earth hemispheres at 12am on 01/01/2015 superimposed onto a map of the Earth.

This data is given in the geographic coordinate system with each latitude and longitude value corresponding to a physical location on the Earth’s surface. Using this coordinate system for our data analysis is unsuitable due to the nature of the data we are using. Our data is inherently linked to Earth’s magnetic field and its position and, since the Earth’s geographic and magnetic poles do not align, it makes little sense to use a coordinate system based around an axis which is essentially independent from our dataset.

Initially we converted the SEC data from Geographic to Magnetic coordinates, a coordinate system which sets the Z-axis parallel to the Earth’s magnetic dipole, following the movement of the dipole over time. Some of this data can be seen in Figure 5 which displays the same currents from Figure 4 converted to magnetic coordinates and projected onto a polar plot.

Ultimately we chose to not use the magnetic coordinate system as, although it is in the reference frame of the Earth’s dipole, it does not account for the exact position of the Earth’s magnetic field lines and so is unsuitable to use when attempting to compare conjugate currents in both hemispheres. Additionally this system is unsuitable for correcting for diurnal asymmetries as the coordinates are given in reference to their physical longitude on the Earth’s surface and not in reference to the Earth’s magnetic field.

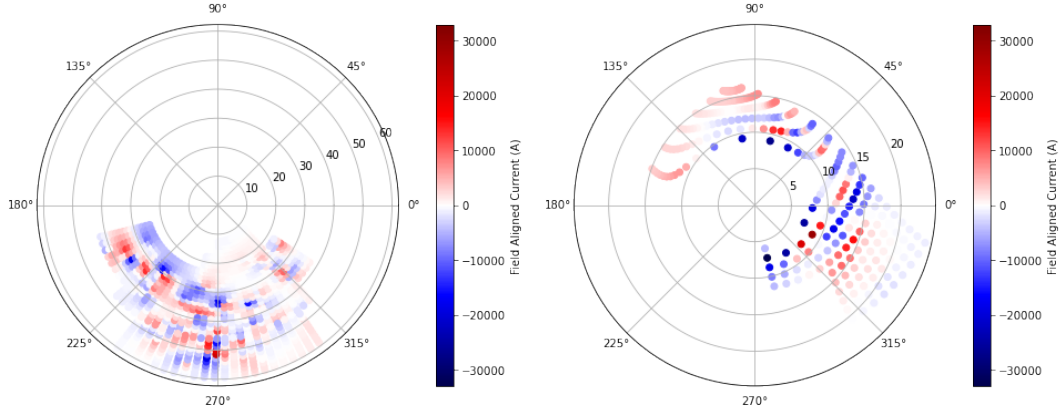


**Figure 5.** SEC field-aligned current amplitudes in the Earth’s North (left) and South (right) Hemispheres at 12am on 01/01/2015, converted to the magnetic coordinate system and projected onto the Earth’s poles.  $0^\circ$  lies on the prime meridian line.

In order to ensure that data from both hemispheres could be accurately compared, we used the Altitude-Adjusted Corrected Geomagnetic (AACGM) coordinate system (Shepherd 2014) to convert the data from geographic coordinates using the AACGM-v2 python library (Burrell, Meeren, and Laundal 2020). AACGM coordinates provide a framework for representing geomagnetic coordinates adjusted for variations in the Earth’s magnetic field, ensuring that conjugate coordinates in both hemispheres can be compared irrespective of their geographic latitudes and longitudes. Additionally we convert the data to Magnetic Local Time (MLT) coordinates, which is defined by the position of the sun, ensuring that the data can be compared by their position relative to the Earth’s magnetosphere and not to the current rotation of the Earth, thus controlling for any diurnal effects.

Converting the data in Figure 5 to the AACGM coordinate system and plotting the values from the perspective of each pole produces the plots in Figure 6. We see from this figure that the Northern Hemisphere contains data with a far larger range of latitudes, between approximately  $0^\circ$  and  $50^\circ$  from the magnetic North pole, while the Southern Hemisphere data ranges between  $10^\circ$  and  $30^\circ$  from the South pole. While these exact ranges will vary due to how AACGM coordinates are calculated with respect to time, this displays roughly the data ranges we will be able to compare with this dataset, and indicates we will not have data over the pole in the Southern Hemisphere.



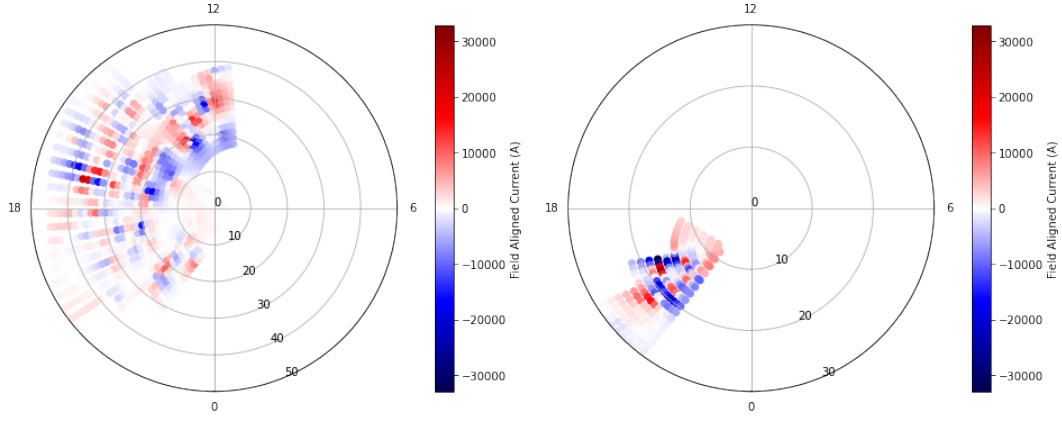


**Figure 6.** SEC field-aligned current amplitudes in the Earth’s North (left) and South (right) Hemispheres at 12am on 01/01/2015, converted to the AACGM coordinate system and projected onto the Earth’s poles. Radial units are in hours with 12 indicating noon with the sun facing the Earth.

The reason that the AACGM MLT coordinate system is suitable for hemispheric comparisons is due to how it removes the effects of known asymmetries in the Earth’s magnetic field. Diurnal asymmetries are standardised via the use of MTL, ensuring that our coordinates are given in a context where they can be compared irrespective of they time of observation. Asymmetry from IMF  $B_y$  will not influence hemispheric comparisons under AACGM coordinates as conjugate points in the Earth’s magnetic field will be mapped to the same point in each hemisphere. With these asymmetries accounted for, we will be able to investigate the differences in the currents in both hemispheres from a baseline position we are able to rule out the factors from previously observed asymmetries.

With the data converted to AACGM coordinates we are able to average over specific time spans, such as a day, to compile the data over the entire 24 hours of the MTL reference frame, by infilling each data point on a map at its given time and latitude. This will be done by averaging the data into bins separated by MLT hours and degrees of latitude, to standardise the data over each day so that they can be compared fairly. The averaged map can be seen for the first day of our dataset in Figure 7. This can be further averaged over larger time spans to account for anomalies and to ensure North and South hemispheric data can be compared more accurately. We do this by taking data around equinoxes where the average current magnitudes in both hemispheres should be equal, due to the incident solar radiation being equal in both hemispheres. However, as our dataset is missing data for some dates in the Southern Hemisphere, we take the largest contiguous range of data either side of each equinox for our comparisons.

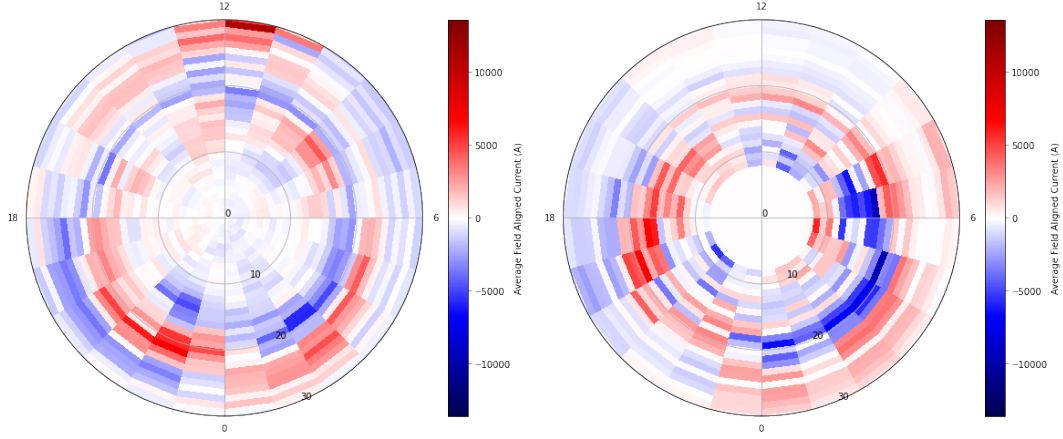


**Figure 7.** SEC field-aligned current amplitudes Earth’s North (left) and South (right) Hemispheres converted to AACGM MLT coordinates and mapped over the entire day of 01/01/2015.

The conversion from geomagnetic to AACGM can produce errors of up to 50km in the latitude and longitude of coordinates near the Earth’s auroral and polar regions (Shepherd 2014) due to the difficulty of perfectly modeling the Earth’s magnetic field at any given time in the past. As the majority of our data lies near the poles, this will have to be taken into account when analysing our results.

Additionally we are able to interpret our data through use of the Asymmetry Index which was originally to quantify the differences in electron density measured in the Earth’s hemispheres (Hong et al. 2021, Wang, Zou, and Cai 2023), but we generalise in order to compare the Earth’s field-aligned currents. Once the data are formatted correctly we are able to use the Asymmetry Index, AI,

$$AI = \frac{2(N - S)}{N + S} \quad (1)$$

to quantify the asymmetry in the field strength between both hemispheres. Here  $N$  and  $S$  are the current amplitudes in the Northern and Southern Hemispheres respectively. This formula calculates a ratio of field strengths where 2 represents total Northern dominance, and  $-2$  total Southern dominance. This index will be used to calculate the hemispheric ratio both temporally, with daily averages over the entire dataset, and spatially for binned data on single days. This will allow us to analyse long term trends as well as see any potential finer structures that may appear in the data.

As  $N$  and  $S$  are required to be of the same sign for this ratio to be accurate, and due to AACGM coordinates having inherent errors near the Earth’s poles, we will have to take the absolute value of the current at each point when calculating the Asymmetry Index to account for conjugate coordinates where the signs are opposite due to conversion errors. While this could result in a loss of information, the magnitude of the Asymmetry Index will still accurately reflect the data, we found this to be an issue only in small portions of the data, approximately  $\sim 7\%$ , and predominantly on the borders between current regions.

### 3 Results and Discussion

Initially we took the average of the data from each day, averaging over all times, latitudes, and longitudes in the years 2015 and 2016 as shown in Figure 8. Though the data displayed in this Figure itself is not sufficient in comparing the Earth’s two hemi-

spheres, as the Northern Hemisphere contains data from a wider range of latitudes, meaning the averages do not directly relate. Additionally small scale features cannot be resolved from these averages and so more data manipulation is required.

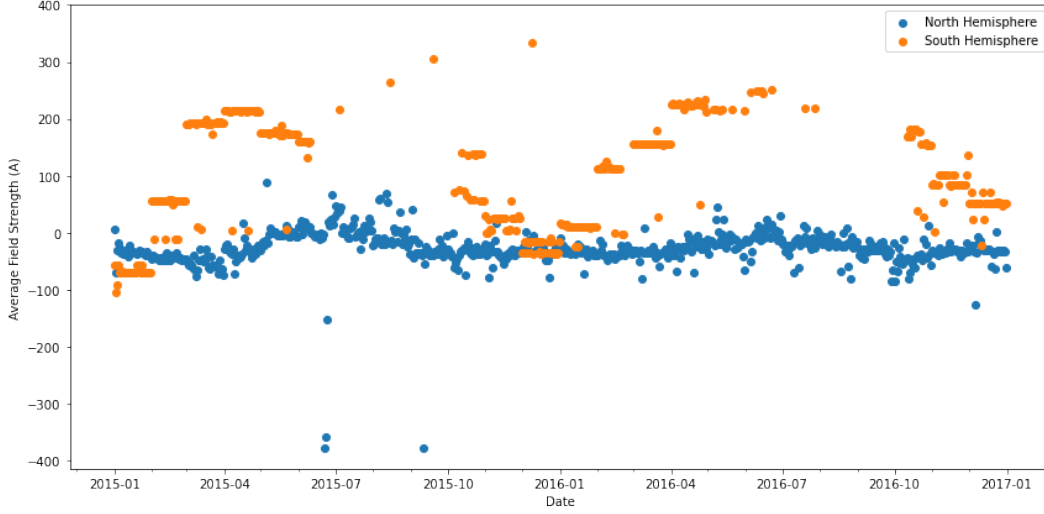


**Figure 8.** Daily average current magnitudes in the Earth’s North and South Hemispheres over the years 2015 - 2016.

Using the average current magnitudes each day we are able to find the Asymmetry Index of the SEC data using Equation 1, this data is displayed in Figure 9. From this we see more positive values for the Asymmetry Index during Northern summer when the current magnitudes are expected to be higher and more negative values during Southern summer for the opposite reasons. The average value for the Asymmetry index over this time frame is  $-0.177$ , while this may indicate a Southern bias to the current magnitudes this is likely not the case as we are missing large portions of the data from Southern winter where the Asymmetry Index is expected to be positive due to seasonal asymmetries, and so this value likely cannot be properly compared to other observations.

We used the Levenberg-Marquardt algorithm (Levenberg 1944, Marquardt 1963) to solve the non-linear least squares problem using the Scipy Python library (Virtanen et al. 2020), we fit a sine curve to this data, giving values of the form,

$$AI = a \sin(bx + c) + d \quad (2)$$

where  $a = 0.389$ ,  $b = 2\pi/0.934Yr$ ,  $c = -2\pi/0.214Yr$  and  $d = -0.0564$ , though these values may not be comparable to other datasets due to the gaps in southern Hemisphere data. The horizontal offset,  $c$ , at  $\sim 0.2$  Years, places the highest points of the curve at the summer solstices and the lowest points at the winter solstices, further reflecting past data (J. C. Coxon et al. 2016) indicating the asymmetries in the ionosphere from seasonal variation. The curve’s vertical offset being close to zero suggests that overall magnitudes between the hemispheres is roughly average over our 2 year time period potentially contradicting observations from J. C. Coxon et al. 2016, where the average Northern currents were found to be on average higher. With an amplitude of  $\sim 0.4$ , we see that the variance in the majority of average daily values is lower than past observations by J. Coxon et al. 2024 which gives an amplitude of  $\sim 0.8$  for the Asymmetry Index in data from AMPERE. The period of this curve is as expected, with roughly one sine wave per year, the fact that our calculated period is not exactly 1Yr is likely due to the missing data during Southern winter.

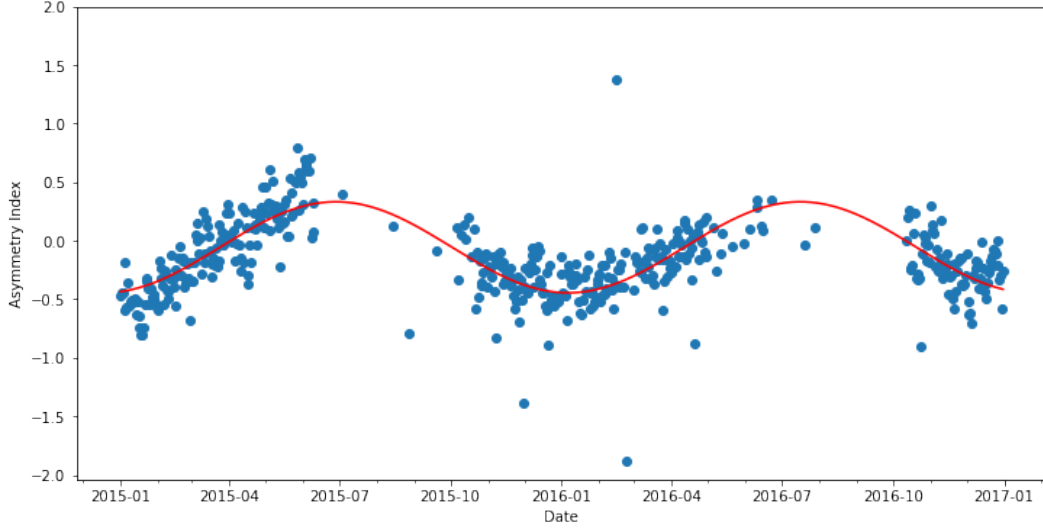


**Figure 9.** Asymmetry Index of the daily currents in the Earth’s North and South Hemispheres over the years 2015 - 2016. The red line indicates the sine curve fitted to the data.

Taking the daily data and converting the coordinates to AACGM we are able to use MLT to rotate the coordinates around the reference frame of the Earth’s magnetosphere, allowing for the data to be compiled and averaged over any given time period. This can be seen in Figure 10 which displays the SEC currents for the Northern Hemisphere over the entire 2015 to 2016 dataset. As bins become physically larger when moving toward the equator there is the potential for equatorial bins to represent the average of more data points, however as the majority of our dataset is near the poles we allow this compromise as it allows for a higher resolution nearer the poles where our data analysis will have more weight. A figure has not been compiled in this manner for the Southern Hemisphere due to the lack of data availability in the south making comparisons over the entire timeframe unfeasible.

Figure 10 clearly displays the separate regions of positive and negative currents at the poles with the central region 1 currents around  $20^\circ$  from the pole, with positive upwards currents to the left close to 18 hours and negative downward currents to the right close to 6 hours. The opposite is true for region 2 currents which lie at roughly  $30^\circ$  from the pole. The borders between the positive and negative sections of these regions appears to be offset by roughly 1-2 hours clockwise from the angle expected in a low IMF  $B_y$  case, which should be inline with the sun at 12 hours (Davey et al. 2012), this indicates an average positive value in the  $B_y$  component of the Earth’s ionosphere over the duration of this dataset.

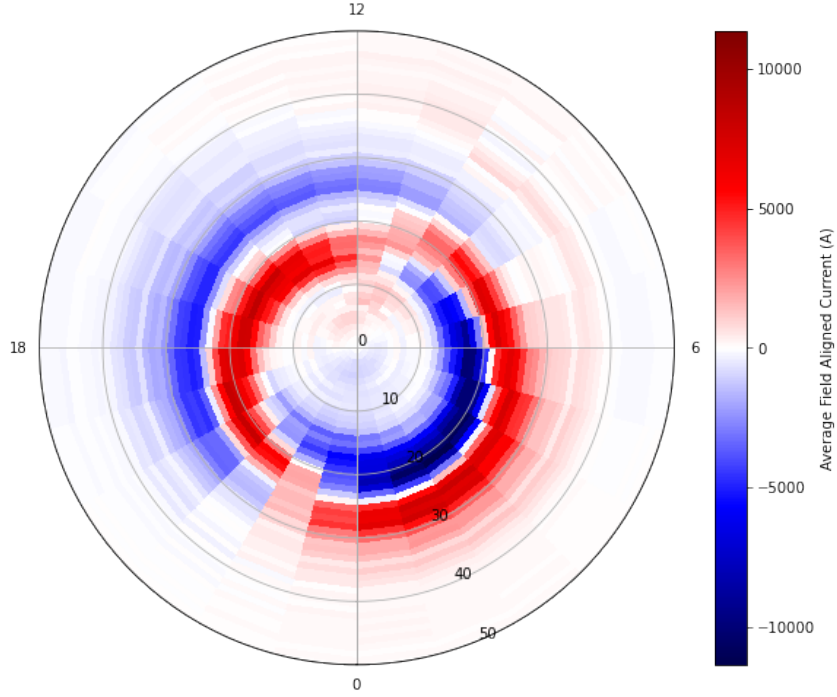


**Figure 10.** Current amplitudes in the Earth's North Hemisphere averaged over the years 2015 - 2016.

It should be noted that the units here are still measured in Amperes (A) as all data manipulation done was simple averages, meaning the values given are essentially the mean field-aligned current for that given bin. This does result in physically larger bins, nearer the equator, having the potential to sample more data for their averages, though given the distribution of our data and the large quantity of data we average over this is not expected to cause any issues. Additionally due to how the Asymmetry Index is calculated, the size of each bin will have no effect on the calculated ratio.

In order to compare the data from both hemispheres we graph over the largest contiguous time spans over each equinox. For this dataset this is only possible for the spring equinoxes on March 20th 2015/2016 as the autumn equinoxes do not have enough southern data for a meaningful comparison. Due to this we will compare data for the 2015 spring equinox over 01/01/2015 and 08/06/2015, and for the 2016 equinox over 01/03/2016 and 10/04/2016. While the timescales used for each of these comparisons are quite large, taking place over roughly 6 months in 2015 vs 1 month in 2016, as the March equinox lies at the centre of each we should be able to avoid interference from seasonal asymmetries in both cases. Additionally, if we are able to produce data which leads to the same conclusion over two different timescales we can be more confident in the results and their potential interpretations.

Data for the 2015 equinox, with Southern data inverted, is displayed in Figure 11 which, like Figure 10, clearly shows the regions of positive and negative current for the hemispheres, with both having roughly the same angle between the positive and negative regions. Additionally the regions of current appear more uniform and structured in the Northern Hemisphere with more clearer region boundaries and fewer areas of low current. While this may be a reflection of real life phenomenon, it is more likely to be influenced by the lower quality data collection available in the Southern Hemisphere, which would result in fewer samples per bin of data, potentially allowing for data in some bins

to be influenced more by smaller sets of data, we see a similar effect in the patchy data visible in our single day plots in Figure 7. A higher quality ground-based Southern Hemisphere dataset would be required to confirm this hypothesis as it is not reflected in space-based data.

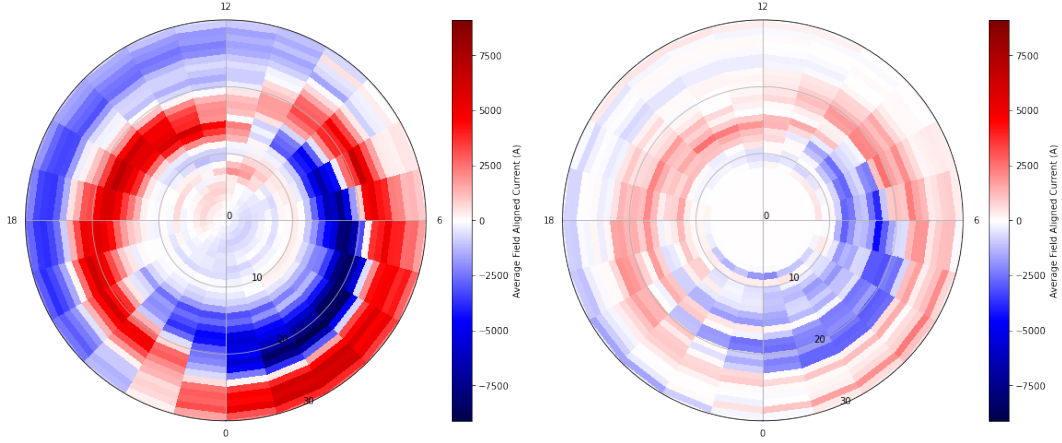


**Figure 11.** Average current amplitudes in the Earth’s North (left) and South (right) Hemispheres over the 2015 March solstice between 01/01/2015 and 08/06/2015.

Figure 11 also indicates higher current magnitudes in the Northern Hemisphere which corroborates data from J. C. Coxon et al. 2016. The maximum field-aligned currents measured in the North and South Hemispheres respectively are 6980A and 2539A, while the lowest measured currents are  $-9107\text{A}$  and  $-4340\text{A}$ . On average, current values were 3.4 times higher in the Northern Hemisphere than in the South.

We use Equation 1 to calculate the Asymmetry Index between the currents in both hemispheres, as previously mentioned we take the absolute current values for this calculation, these values are displayed in Figure 12. From this we can see clearly the Northern bias in current as the majority of values take a positive value and thus indicate a higher current magnitude in the north. The largest group of negative values appears around  $10^\circ$  from the pole at the side of the Earth facing away from the sun. The average Asymmetry Index over this equinox was 0.786, displaying the clear Northern bias in the field-aligned current magnitudes.

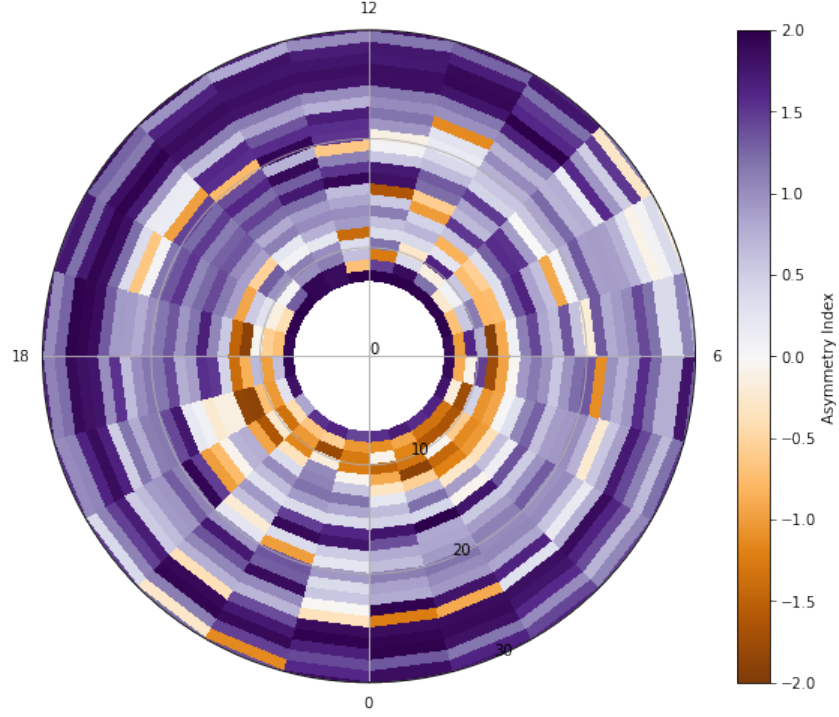


**Figure 12.** Asymmetry Index of the absolute current amplitudes between the Earth's hemispheres over the 2015 March solstice between 01/01/2015 and 08/06/2015

We also calculated averages over the 2016 spring equinox using the same technique, displaying the results in Figure 13. Again this Figure displays the different regions of current clearly but with the current regions rotated clockwise when compared with what is seen in Figure 10 or Figure 11, potentially indicating the IMF  $B_y$  field was stronger over this period of time. The Figure also displays equally as uniform current regions in both hemispheres as seen over the 2015 spring equinox in Figure 11.

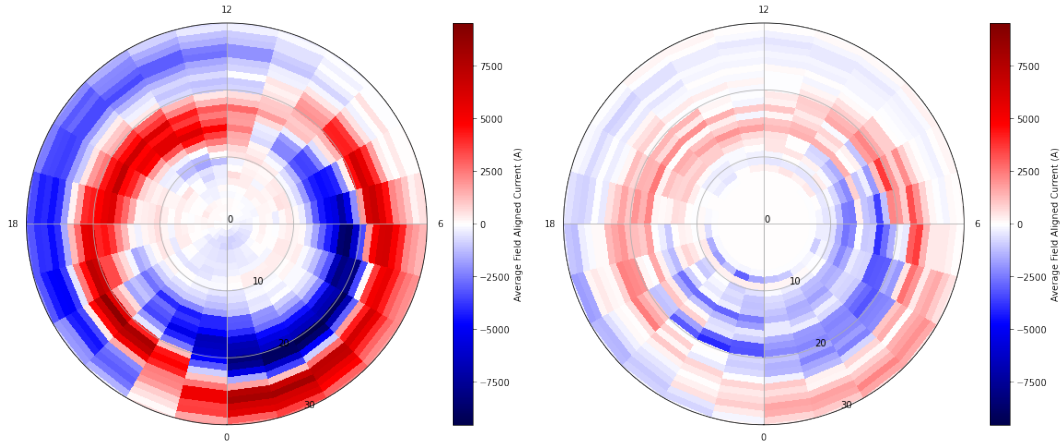


**Figure 13.** Average current amplitudes in the Earth's North (left) and South (right) hemispheres over the 2016 March solstice between 01/03/2016 and 10/04/2016.



The highest average field-aligned current were 8875A and 3709A in the North and South Hemispheres respectively, with the lowest average values of  $-9536\text{A}$  and  $-3979\text{A}$ . Average current values in the North were 3.3 times higher than in the South.

Figure 14 displays the Asymmetry Index over the 2016 equinox. The majority of values are again positive indicating higher magnitudes of current in the Northern Hemisphere, consistent with 12. Additionally we see the largest region of negative currents at  $10^\circ$  at the night side of the Earth. The average Asymmetry Index over this equinox was 0.789, again indicating the Northern bias in the current magnitudes.

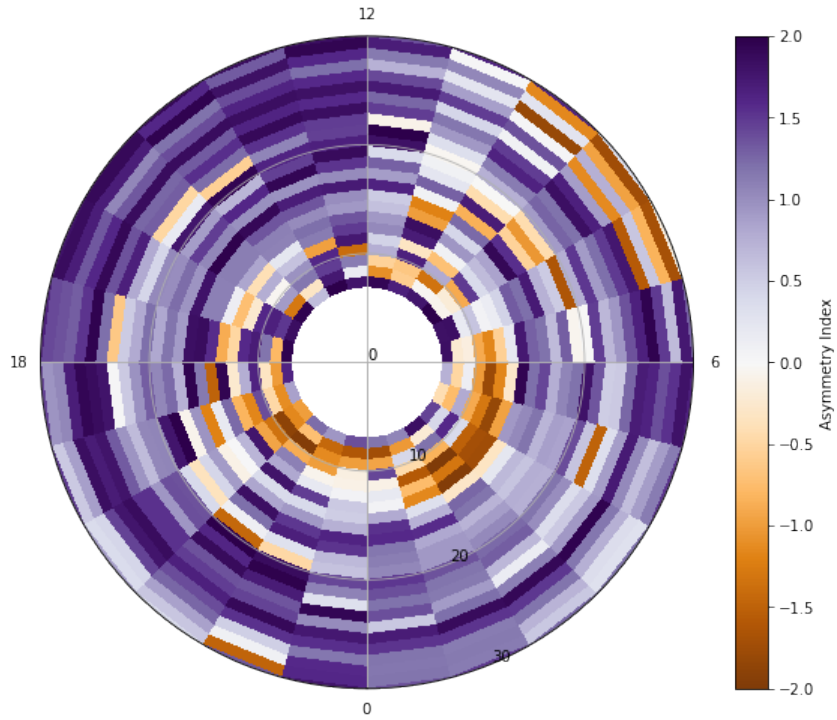


**Figure 14.** Asymmetry Index of the absolute current amplitudes between the Earth's hemispheres over the 2016 March solstice between 01/03/2016 and 10/04/2016.

Despite our data, both over the whole 2 years and over the individual spring equinoxes, appearing to display rotations consistent with an average positive IMF  $B_y$  fields, space-based observations display no overall bias in this component of the IMF as seen in Figure 15 (Papitashvili and King 2020).



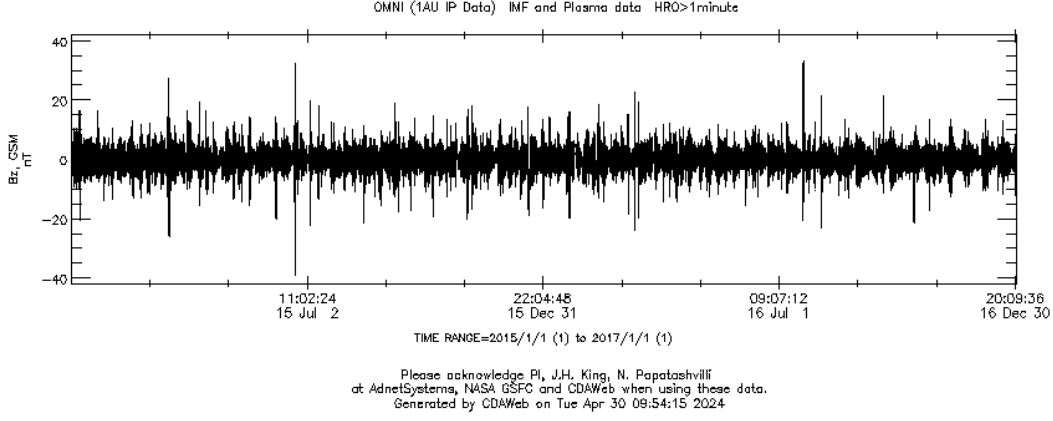


**Figure 15.** IMF  $B_y$  from NASA's OMNI dataset between 2015 - 2016 (Papatashvili and King 2020).

The Asymmetry Index being mostly positive in the data over the spring equinoxes appears to contradict the overall trend from Figure 9, where the average Asymmetry Index was close to zero. This may be explained due to the fact that we do not have graphs from autumn equinoxes which may have negative Asymmetry Indexes to balance out the data, though this would require ground-based data from Southern winter to confirm.

#### 4 Conclusions

Over both spring equinoxes the Northern Hemisphere field-aligned currents to be  $\sim 3$  times higher than Southern Hemisphere currents, over twice the measured difference from previous space-based data (J. C. Coxon et al. 2016, Workayehu, Vanhamäki, and Aikio 2019). The groups of negative Asymmetry Index values at  $\sim 10^\circ$  visible in both Figure 12 and Figure 14 may suggest each hemisphere experiences a slight diurnal effect causing night side polar regions to experience higher currents in the Southern Hemisphere.

From Figure 9 we found the Asymmetry Index had a period of 0.934Yr while expected seasonal asymmetries predict this value should be closer to 1Yr. Preliminary data from J. Coxon et al. 2024 displays a similar phenomenon with the period not consistently following expected models, with the residual difference between models and expected data taking the form of a sine wave. A possible explanation for this may be the effect that the solar cycle has on the Earth's magnetosphere, which may result in longer or shorter periods depending on the current phase of the sun, this may be evident here as our dataset occurs immediately after solar maximum. Although any investigation of this potential phenomena would require a complete dataset over at least one full solar cycle.

The SEC dataset appears to indicate the  $B_y$  component of the IMF was positive on average due to the data displaying a clockwise rotation of the polar current regions by  $\sim 1$ -2 hours over the low  $B_y$  case. However, as there was no overall trend in the measured IMF  $B_y$  over the timeline of our dataset, these rotations must have been induced in some capacity by the Earth's atmosphere.

While the majority of our results agree broadly with past observations, certain differences, such as our lower amplitude of the Asymmetry Index, at  $\sim 0.4$  (Figure 9) than calculated by J. Coxon et al. 2024, at  $\sim 0.8$ , these differences may be explained due to our use of ground-based data over space-based observations which allows our results to be influenced by the Earth's atmosphere in addition to all other sources of interference. Workayehu, Vanhamäki, and Aikio 2019 suggests, as higher currents in the Northern Hemi-

sphere are only present under low-activity conditions, that local ionospheric conditions may play a role in explaining this asymmetry. Another possible explanation from Pourkarim and Knudsen 2024 indicates the Ionospheric Pedersen conductance to be consistently higher in the Northern Hemisphere which may influence ground-based observation, though further investigation would be needed to confirm a direct link.

Controlling for these other potential sources of asymmetry in further investigations may help to elucidate the sources of the unknown asymmetries in the currents of the Earth's magnetosphere as well as demonstrate the effect the atmosphere has on these currents before they can be detected by ground-based observation.

## References

- Amm, O. and A. Viljanen (June 1999). "Ionospheric disturbance magnetic field continuation from the ground to the ionosphere using spherical elementary current systems". In: *Earth, Planets and Space* 51.6, pp. 431–440. DOI: 10.1186/BF03352247.
- Burrell, Angeline, Christer van der Meeren, and Karl M. Laundal (Jan. 2020). *aburrell/aacgm2: Version 2.6.0*. Version 2.6.0. DOI: 10.5281/zenodo.3598705. URL: <https://doi.org/10.5281/zenodo.3598705>.
- Cowley, S. W. H. (Jan. 2000). "TUTORIAL: Magnetosphere-Ionosphere Interactions: A Tutorial Review". In: *Geophysical Monograph Series* 118, p. 91. DOI: 10.1029/GM118p0091.
- Cowley, Stanley W. H. (2007). "Magnetosphere of the Earth". In: *Encyclopedia of Geomagnetism and Paleomagnetism*. Ed. by David Gubbins and Emilio Herrero-Bervera. Dordrecht: Springer Netherlands, pp. 656–664. ISBN: 978-1-4020-4423-6. DOI: 10.1007/978-1-4020-4423-6\_205. URL: [https://doi.org/10.1007/978-1-4020-4423-6\\_205](https://doi.org/10.1007/978-1-4020-4423-6_205).
- Coxon, J. et al. (Apr. 2024). "The asymmetry towards stronger Birkeland currents in the Northern Hemisphere". In: *EGU General Assembly 2024, Vienna, Austria*. URL: <https://doi.org/10.5194/egusphere-egu24-11337>.
- Coxon, J. C. et al. (May 2016). "Seasonal and diurnal variations in AMPERE observations of the Birkeland currents compared to modeled results". In: *Journal of Geophysical Research (Space Physics)* 121.5, pp. 4027–4040. DOI: 10.1002/2015JA022050. arXiv: 1701.02961 [physics.space-ph].
- Coxon, John C. et al. (Feb. 2022). "Distributions of Birkeland Current Density Observed by AMPERE are Heavy-Tailed or Long-Tailed". In: *Journal of Geophysical Research (Space Physics)* 127.2, e2021JA029801, e2021JA029801. DOI: 10.1029/2021JA029801.
- Davey, E. A. et al. (July 2012). "The orientation and current density of the magnetotail current sheet: A statistical study of the effect of geomagnetic conditions". In: *Journal of Geophysical Research (Space Physics)* 117.A7, A07217, A07217. DOI: 10.1029/2012JA017715.
- Hong, Yu et al. (Nov. 2021). "Impacts of Different Causes on the Inter-Hemispheric Asymmetry of Ionosphere-Thermosphere System at Mid- and High-Latitudes: GITM Simulations". In: *Space Weather* 19.11, e2021SW002856, e2021SW002856. DOI: 10.1029/2021SW002856.
- Levenberg, Kenneth (1944). "A METHOD FOR THE SOLUTION OF CERTAIN NON – LINEAR PROBLEMS IN LEAST SQUARES". In: *Quarterly of Applied Mathematics* 2, pp. 164–168. URL: <https://api.semanticscholar.org/CorpusID:124308544>.
- Marquardt, Donald W. (1963). "An Algorithm for Least-Squares Estimation of Nonlinear Parameters". In: *Journal of the Society for Industrial and Applied Mathematics* 11.2, pp. 431–441. DOI: 10.1137/0111030. eprint: <https://doi.org/10.1137/0111030>. URL: <https://doi.org/10.1137/0111030>.
- Merrill, R.T., M.W. McElhinny, and P.L. McFadden (1998). *The Magnetic Field of the Earth: Paleomagnetism, the Core, and the Deep Mantle*. International geophysics

- series. Academic Press. ISBN: 9780124912465. URL: <https://books.google.co.uk/books?id=96AP14nK91IC>.
- Papitashvili, Natalia E. and Joseph H. King (2020). *OMNI Hourly Data [Data Set]*. NASA Space Physics Data Facility. DOI: <https://doi.org/10.48322/1shr-ht18>. URL: <https://cdaweb.gsfc.nasa.gov>.
- Pourkarim, P. and D. Knudsen (Apr. 2024). “Ionospheric Conductance Derived from Satellite Measurements: Limitations and Implications”. In: *EGU General Assembly 2024, Vienna, Austria*. URL: <https://doi.org/10.5194/egusphere-egu24-6566>, %202024.
- Shepherd, S. G. (2014). “Altitude-adjusted corrected geomagnetic coordinates: Definition and functional approximations”. In: *Journal of Geophysical Research: Space Physics* 119.9, pp. 7501–7521. DOI: <https://doi.org/10.1002/2014JA020264>. eprint: <https://agupubs.onlinelibrary.wiley.com/doi/pdf/10.1002/2014JA020264>. URL: <https://agupubs.onlinelibrary.wiley.com/doi/abs/10.1002/2014JA020264>.
- Virtanen, Pauli et al. (2020). “SciPy 1.0: Fundamental Algorithms for Scientific Computing in Python”. In: *Nature Methods* 17, pp. 261–272. DOI: 10.1038/s41592-019-0686-2.
- Wang, Zihan, Shasha Zou, and Xuguang Cai (Oct. 2023). “Hemispheric Asymmetries in Thermospheric Composition and Temperature: GOLD Observations”. In: *Journal of Geophysical Research (Space Physics)* 128.10, e2023JA031868, e2023JA031868. DOI: 10.1029/2023JA031868.
- Weimer, D. R. (July 2001). “Maps of ionospheric field-aligned currents as a function of the interplanetary magnetic field derived from Dynamics Explorer 2 data”. In: 106.A7, pp. 12889–12902. DOI: 10.1029/2000JA000295.
- Weygand, J. M. et al. (June 2023). “Interhemispheric Asymmetry Due To IMF By Within the Cusp Spherical Elementary Currents”. In: *Journal of Geophysical Research (Space Physics)* 128.6, e2023JA031430, e2023JA031430. DOI: 10.1029/2023JA031430.
- Weygand, James M. et al. (Mar. 2011). “Application and validation of the spherical elementary currents systems technique for deriving ionospheric equivalent currents with the North American and Greenland ground magnetometer arrays”. In: *Journal of Geophysical Research (Space Physics)* 116.A3, A03305, A03305. DOI: 10.1029/2010JA016177.
- Workayehu, A. B., H. Vanhamäki, and A. T. Aikio (Aug. 2019). “Field-Aligned and Horizontal Currents in the Northern and Southern Hemispheres From the Swarm Satellite”. In: *Journal of Geophysical Research (Space Physics)* 124.8, pp. 7231–7246. DOI: 10.1029/2019JA026835.
- (Oct. 2020). “Seasonal Effect on Hemispheric Asymmetry in Ionospheric Horizontal and Field-Aligned Currents”. In: *Journal of Geophysical Research (Space Physics)* 125.10, e28051, e28051. DOI: 10.1029/2020JA028051.1002/essoar.10502656.1.
- Workayehu, A. B., H. Vanhamäki, A. T. Aikio, and S. G. Shepherd (Oct. 2021). “Effect of Interplanetary Magnetic Field on Hemispheric Asymmetry in Ionospheric Horizontal and Field-Aligned Currents During Different Seasons”. In: *Journal of Geophysical Research (Space Physics)* 126.10, e29475, e29475. DOI: 10.1029/2021JA029475.1002/essoar.10506875.1.